J. Anat. (2003) **202**, pp315–325

Histological and immunohistological investigation of the lymphoid tissue in normal and mycobacteria-affected specimens of the Rufous Hare-wallaby (*Lagorchestes hirsutus*)

L. J. Young,[1,4] R. McFarlane,[2] A. L. Slender[1] and E. M. Deane[3,4]

[1]*School of Science, Food and Horticulture, University of Western Sydney, NSW, Australia*
[2]*Animal Health Department, Alice Springs Desert Park, PO Box 2130 Alice Springs, Northern Territory, Australia*
[3]*Division of Environmental and Life Sciences, Macquarie University, NSW, Australia 2109*
[4]*Co-Operative Research Centre for Marsupial Conservation and Management, Macquarie University, NSW, Australia*

Abstract

The histology of the spleen, lymph nodes, Gut-associated lymphoid tissue (GALT) and Bronchus-associated lymphoid tissue (BALT) are described for samples collected opportunistically from healthy and mycobacteria-affected specimens of the endangered marsupial *Lagorchestes hirsutus*, the Rufous Hare-wallaby. The structural elements, organization and distribution of T and B lymphocytes determined by immunohistological techniques using species cross-reactive antibodies in the lymph nodes, spleen and GALT of this species demonstrated lymphoid cell distributions that were consistent with other marsupial and eutherian mammals. The tissues of animals identified as acid-fast positive displayed immunopathology consistent with the responses to intracellular bacteria displayed in some eutherian mammals and included the presence of focal lesions, giant cells in the lung and lymphoid aggregations situated adjacent to blood and airway vessels. This is the first study to describe the lymphoid tissue of this rare macropod species and the first to document the tissue bed response to mycobacteria.

Key words acid-fast; BALT; GALT; Mala; marsupial.

Introduction

The Rufous Hare-wallaby or Mala (*Lagorchestes hirsutus*) is one of four species of hare-wallaby from the marsupial genus *Lagorchestes* (subfamily *Macropodinae*) (Maxwell et al. 1996; Kirsch et al. 1997). These animals are amongst the smallest members of the macropod family and were once abundant in the spinifex areas of Australia. However, owing to factors such as the predatory impact of introduced species and changes in fire regimes that altered vegetation patterns (Bolton & Latz, 1978), the Mala is now critically endangered and is classified as 'extinct in the wild' (Maxwell et al. 1996). Island populations currently exist off the Western Australian Coast on Bernier and Dorre Islands, but mainland numbers are limited to a small, managed colony of animals in predator-proof enclosures in the Tanami Desert of the Northern Territory (Johnson, 1988). Moreover, this colony appears to be particularly susceptible to mycobacterial infection, a significant problem for such an endangered group (Buddle & Young, 2000).

The endangered status of this species has clearly limited the opportunity for immunological research on these animals, as has the lack of marsupial-specific reagents.

In the last 10 years, the situation has improved with the advent of species cross-reactive antibodies that recognize lymphocyte populations across a range of mammalian species.

These antibodies, developed to conserved regions of human lymphocyte cell-surface markers (Mason et al. 1989), have successfully recognized lymphocytes in eutherian mammals such as bovine and equine species (Jones et al. 1993), in a prototherian mammal, the

Correspondence
Dr E. M. Deane, Division of Environmental and Life Sciences, Macquarie University, NSW, Australia 2109. Tel.: 612 98508418; fax: 612 98509671; e-mail: edeane@els.mq.edu.au

Accepted for publication *12 December 2002*

Table 1 Animal details and the source of individual tissues examined in this study

No.	Sample reference number/sex/age	Reason for being killed	Autopsy details	Acid fast result	Tissue samples
1	241 female/8 years	Mycobacterial disease	Osteomyelitis, osteoarthritis, cream coloured pus	Positive	mesenteric and thyroid-associated lymph nodes, gut, lung, spleen
2	89518722 female/5 years	Trauma injury*	Osteomyelitis, osteoarthritis	Positive	hepatic lymph nodule, lung, spleen
3	960106 female/8 years	Normal husbandry	No gross lesions, mild gut pathology, no parasites	Positive	lung, duodenal lymph nodes, spleen
4	970500 female/8 years	Normal husbandry	No gross lesions, cestodes	Positive	adrenal lymph node, spleen
5	970510 female/7 years	Normal husbandry	No autopsy	Negative	gut, lung, spleen
6	990068 unknown	Trauma injury*	No autopsy	Positive	lung, spleen, brain
7	990107 male/1 year	Normal husbandry	No gross lesions, cestodes	Negative	gut, spleen
8	990109 unknown	unknown	No autopsy	Negative	spleen

*Fractured femur most likely due to underlying mycobacterial infection.

platypus, *Ornithorhynchus anatinus* (Connolly et al. 1999), and in a range of marsupials including the brushtail possum, *Trichosurus vulpecula* (Jones et al. 1993; Baker et al. 1999), the ringtail possum, *Pseudocheirus peregrinus*, and the Tammar wallaby, *Macropus eugenii* (Hemsley et al. 1995; Old & Deane, 2002a), the koala, *Phascolarctus cinereus* (Hemsley et al. 1995; Canfield et al. 1996), the Brazilian white-belly opossum, *Didelphis albiventris* (Coutinho et al. 1995), the northern brown bandicoot, *Isoodon macrourus* (Cisternas & Armati, 2000; Old & Deane, 2002b), and the eastern grey kangaroo, *Macropus giganteus* (Old & Deane, 2001). These studies have confirmed the structural similarity between the three classes of mammals, eutherians (placentals), metatherians (marsupials) and prototherians (monotremes).

To date, there are no reports of the immunobiology of the Rufous Hare-wallaby. The present study documents the histology and immunopathology of the lymphoid tissues of this endangered species based upon samples that were collected opportunistically from animals that were clinically normal, those that were victims of trauma or those with clinically diagnosed mycobacterial disease.

Materials and methods

Sample collection

Samples in this study were opportunistically obtained from a colony of animals originally sourced from the Tanami Desert (NT, Australia) that were kept as a captive breeding population in the Alice Springs Desert Park (NT, Australia). Animals were killed with an overdose of Lethobarb as per standard operating protocols in the Desert Park. Tissue samples were collected from a total of eight animals. Four of these were killed as part of normal husbandry of the collection, aimed at maintaining viable, healthy, representative populations. These four animals were clinically normal at the time of death, although acid-fast bacteria were subsequently detected in some histological sections. Two animals were killed after suffering trauma injury in their enclosures but were otherwise clinically normal at the time. Both were subsequently found to have acid-fast bacteria in their tissue beds. One animal was killed because of overt symptoms of mycobacterial infection. Tissue samples for analysis were removed and immediately placed in 10% neutral-buffered formalin before transport to the laboratory. Table 1 summarizes details of age, sex, sampling sites, health status of the animals at the time of death and the results of acid fast staining.

Histology

Tissue samples were transferred from formalin fixative to ethanol, routinely processed and embedded in paraffin wax (Bancroft & Stevens, 1990). Serial sections of paraffin blocks were cut at a thickness of 4 or 6 μm and applied to aminopropyltriethoxysilane-coated slides. The number of blocks prepared varied according to the size of the available tissue. For lung and liver samples six blocks were prepared, whilst for node the tissue could be successfully encased in one block. Each block was

serially sectioned for further examination. For routine histological and immunohistological staining, sections were deparaffinized through xylene and rehydrated through a graded alcohol series (Celis, 1994). Sections were stained with Harris haematoxylin (Sigma; St Louis, MO, USA) for 30 s and Eosin Y solution (Sigma) for 15 s before dehydration and mounting using Entellen mountant (Merck, Whitehouse, NJ, USA).

Acid-fast screening

Since some of the animal tissue investigated in this study was obtained from animals that were killed due to clinical presentations of osteomyelitis and long bone fractures associated with mycobacterial infection, screening for the presence of acid-fast bacteria was performed on all tissue samples, even those from clinically asymptomatic animals. Paraffin-embedded tissue sections were cut to a thickness of 6 μm, deparaffinized in xylene, rehydrated through a graded ethanol series and rinsed in water, followed by staining with Accustain Acid Fast Staining kit (Sigma Diagnostics®) according to manufacturer's instructions. A commercially purchased tissue section containing mycobacterium species (Sigma) was included in staining protocols as a positive control.

Antibodies and immunohistological technique

Monoclonal antibodies raised to conserved regions of the T lymphocyte surface antigen CD5 (CD5/54) and the B lymphocyte antigen CD79b (B29/123) were supplied as tissue culture supernatants by Dr Margaret Jones of the Leukaemia Research Fund Immunodiagnostics Unit (Oxford, UK). Both antibodies were trialled at dilutions of 1/10 and 1/50 and were found to be optimal at the 1/50 dilution. This dilution was subsequently used for all routine analyses. Negative control samples were run in parallel with all test panels and included mouse IgG_1 for CD5 and IgG_{2b} for CD79b and replacement of both primary and secondary antibodies with PBS to confirm test specificity. A section of Tammar wallaby lymph node was also included as a positive control.

With the exception of the antigen retrieval process, all steps were performed at room temperature (~20 °C) in a humidified container to prevent dehydration of tissue sections. Sections for immunostaining were deparaffinized, dehydrated and equilibrated in phosphate-buffered saline (PBS). Endogenous peroxidase was blocked with 0.6% hydrogen peroxide in 50% methanol/50% PBS (v/v) for 30 min followed by a 5-min wash in PBS. To facilitate antigen exposure, tissue sections were subjected to a microwave treatment using Vector Antigen Unmasking Solution (Vector Laboratories; CA, USA) according to the manufacturer's instructions before sections were transferred to PBS for equilibration. Sections were washed in PBS for 5 min and covered with a 1/50 dilution of horse serum in PBS for 30 min to block non-specific binding sites. Serum solution was removed by gentle tapping of the slides and primary antibodies were immediately applied to the sections that were then incubated for 60 min. Unbound antibody was removed by a 5-min wash with PBS before antibody binding sites were detected using the Vectorstain *E*lite peroxidase kit (Vector Laboratories) in association with the chromagen, diaminobenzidine (DAB).

A universal biotinylated secondary antibody was applied to each section for 30 min followed by 30 min incubation with an avidin and biotinylated horseradish peroxidase complex designed to amplify the target signal. DAB in urea-hydrogen peroxide (Sigma) was added to each section and incubated for 5–8 min to develop the brown precipitate indicative of positive antigen reactivity. To enhance contrast, sections were counterstained with haematoxylin for 30 s, dehydrated through an alcohol series and xylene and mounted. Positive antibody localization was indicated microscopically by a brown stain in the membrane or cytoplasm of cells. Negatively stained sections appeared blue.

Microscopy

Sections were inspected and representative photomicrographs were obtained using either an Olympus CX40 compound light microscope fitted with an SC35 camera or a Zeiss Axiophot 20 microscope fitted with an MC80 camera.

Results

Detection of acid-fast bacteria

The tissues of five out of eight animals investigated in this study stained positive for the presence of acid-fast bacteria (Table 1). Of these, only one animal, number 1, had been clinically diagnosed as suffering from mycobacterial disease. Acid-fast bacteria were, however, detected in duodenal nodules of animal 3 (Fig. 1), in a section of a brain plaque isolated from animal 6, in the

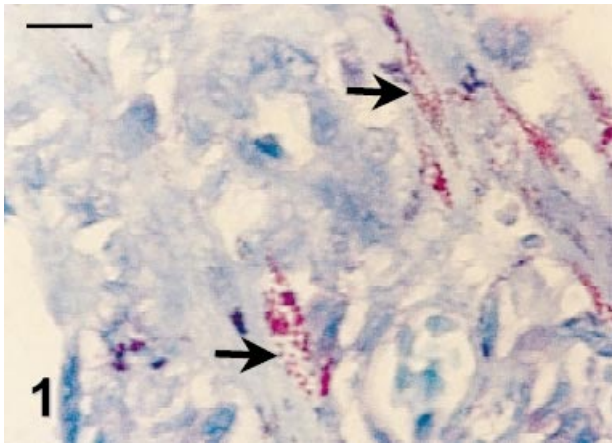

Fig. 1 Acid-fast staining of Mala duodenal nodule. Individual pink-staining bacteria (arrows) are visible in tissue histiocytes. Scale bar = 10 μm.

lymph node and spleen of animal 4, in the spleen and lung of animal 2, and the intestine, mesenteric lymph node and spleen of animal 1. In general, these organisms were localized to histiocytic cells, although a number of tissue sections contained bacteria scattered throughout the tissue parenchyma.

Lymph nodes

Lymph nodes from a variety of anatomical locations from different animals were examined (see Table 1). These included mesenteric nodes, an adrenal-associated node, a thyroid-associated node and an hepatic lymphoid nodule. This was dictated by the opportunistic nature of the collection. All lymph nodes, regardless of anatomical site of origin and acid-fast status, were surrounded by a capsule with an obvious subcapsular sinus. These routinely contained lymphocytes. In all samples the outer capsule was continuous with the trabeculae, which divided the nodes into discrete regions. The lymphatic exit point, the hilus, was also identified in all nodes. Both an outer cortical area and an inner medulla were clearly discernible (Fig. 2a). The cortex of lymph nodes was composed of primary and secondary lymphoid follicles, trabeculae and lymphatic sinuses. In routine histological inspections, the primary follicles were clearly distinguished by their darkly stained lymphocytes and secondary follicles were recognized by their pale-staining germinal centres and contrasting outer coronas. The medullary regions contained extensive sinuses, medullary cords and obvious blood vessels, all separated by connective tissue (Fig. 2b). The organization of the structural elements was similar for all nodes although there were differences in numbers and presence of primary and secondary follicles and the arrangement of medullary elements. In animal 4 the sinus of the adrenal node contained large eosinophilic macrophages and numerous neutrophils were apparent in the subcapsular region of the gut node of animal 1. Both these animals had acid-fast bacteria in their tissue beds.

A paracortical zone that was densely populated with T lymphocytes as demonstrated by anti-CD5 antibody staining (Fig. 2c) was clearly visible in all nodes. In general, CD5-positive cells were present in large numbers in the paracortical zones and were found in low to medium density in the lymphoid follicles. These cells were also scattered in low numbers throughout other regions of the node. In the mesenteric node of acid-fast-positive animal 1, the paracortical area was very large. This node also contained fewer lymphoid follicles than other lymph nodes inspected in this study.

B cells, evidenced by anti-CD79b antibody staining, were the most numerous cell type found in the cortical follicles and were densely collected in the mantle zones of germinal centres (Fig. 2d). The germinal centres of secondary follicles were less intensely stained and contained lower numbers of these cells. Lymphoblasts, mitotic cells and macrophages were present in variable numbers in these regions. Medullary cords and sinuses were visible in all nodes and were very extensive in the thyroid-associated node of animal 1. Medullary cords contained macrophages as well as both CD5- and CD79b-positive lymphocytes. Scattered throughout the lymph node but most prevalent in the cortex were phagocytic histiocytes, easily identified by their white appearance against a darkly stained background.

Spleen

A fibrous capsule surrounded the spleen and enclosed obvious areas of red and white pulp. No distinct cortex or medulla region was apparent. Trabeculae extended inward from the capsule and were diffusely distributed throughout the cellular parenchyma (Fig. 3a). The white pulp of the spleen consisted of both splenic corpuscles (lymphatic nodules) and lymphoid sheaths surrounding arterioles. Lymphatic follicles were distributed throughout the organ and both primary and secondary follicles were identified. Some secondary follicles contained very large germinal centres that were atypical compared with most other samples (Fig. 3b). Lymphatic tissue

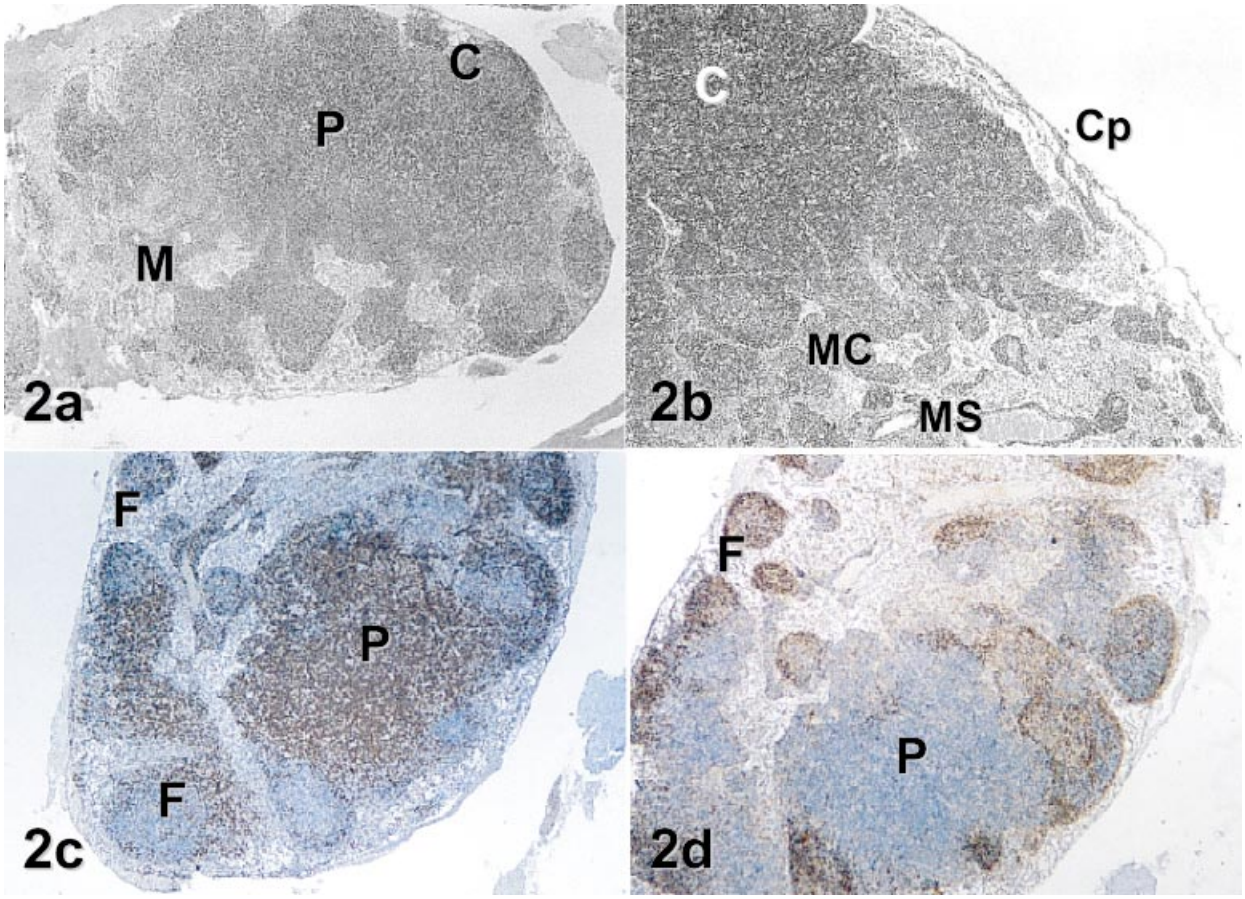

Fig. 2 Mala lymph node structure. (a,b) The basic organization of lymph nodes. The outer cortex (C) and inner medulla (M) separated by an afollicular paracortical (P) region can be seen at low magnification in the gut node in (a) (H&E, ×32). At higher magnification in (b), details of the capsule (Cp), cortex (C) and medullary cords (MC) and sinuses (MS) are more apparent in a section of an adrenal-associated node (H&E, ×40). (c,d) The distribution of T and B lymphocytes within the gut node. In (c), anti-CD5 positively labelled cells densely pack the paracortex (P) and interfollicular regions of the node. Some CD5-positive cells are also visible in the periphery of lymphoid follicles (F) and in the medullary cords (Immunoperoxidase, ×40). (d) The distribution of B cells in a consecutive tissue section. CD79b-positive B cells were most numerous in cortical follicles (F) and were scattered throughout the tissue parenchyma. Note that very little staining of cells within the paracortex (P) is evident with this antibody (Immunoperoxidase, ×40).

surrounding the arteries was present as periarteriolar lymphoid sheaths (PALS) (Fig. 3c).

The red pulp of the spleen was composed of splenic sinuses and cords that were difficult to differentiate in some of the diseased tissue. The red pulp of tissues from apparently healthy animals contained erythrocytes, macrophages, lymphocytes and large cells resembling megakaryocytes and myeloid cell precursors.

Immunohistologically, almost all cells of the PALS stained strongly with anti-CD5 antibody, confirming the abundance of T cells in this area (Fig. 3c). Secondary follicles were stained with this antibody in regions, mainly in areas underlying the mantle. Small numbers of T lymphocytes were also scattered throughout the tissue immediately surrounding the PALS. The B-cell antibody stained almost all cells of the primary splenic follicles and densely stained the corona of the germinal centres (Fig. 3d). Germinal centres of splenic follicles contained sparse numbers of these cells, but also contained lymphoblasts, macrophages, cells with pyknotic nuclei and supporting cells.

In mycobacteria-infected animals, the walls of most blood vessels and venous sinuses appeared to be thickened and, in two samples (1 and 7), extensive fibrosis was apparent. Trabeculae were fibrotic and thickened and were sometimes difficult to distinguish from granulation tissue. Continuous stretches of white pulp were evident surrounding the arterioles and comprised up to 30% of the total splenic volume. In two of these samples (5 and 6), this increased amount of lymphoid tissue

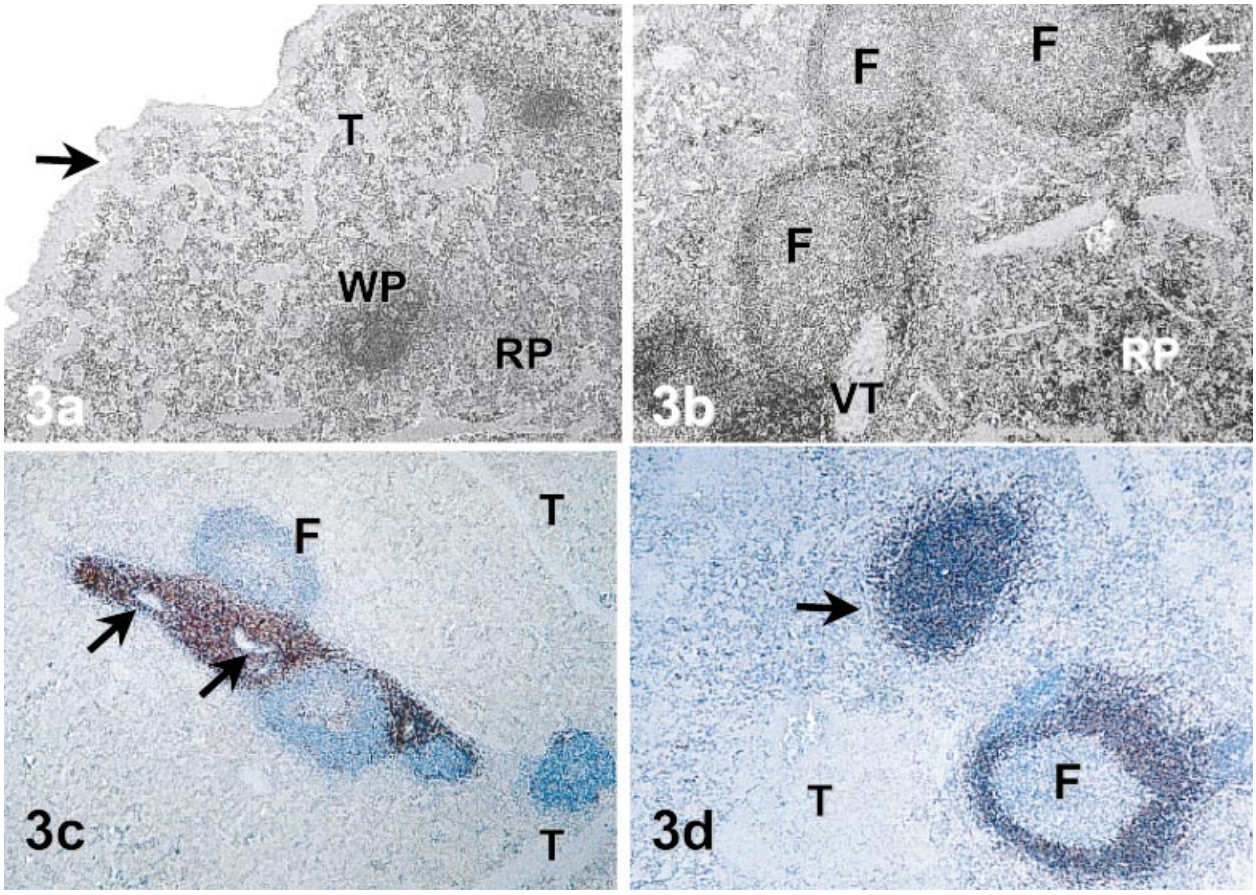

Fig. 3 Histology and Immunohistology of Mala spleen. (a,b) The basic structure of splenic tissue. In (a), a capsule (arrow) with trabeculae (T) extending into the splenic parenchyma surrounds areas of white (WP) and red (RP) pulp (H&E, ×40). In (b), a section from a different animal, an arteriole (arrow), secondary follicles (F) with lighter staining germinal centres, vascular trabeculae (VT) and the cellular nature of the red pulp (RP) can be seen (H&E, ×40). (c,d) The immunohistological staining of white pulp using anti-T-cell and anti-B-cell antibodies. Anti-CD5 T-cell staining is apparent in the PALS in (c). Note the large numbers of T cells surrounding the arterioles (arrow) and the scattering of CD5-positive cells within the germinal centres (Immunoperoxidase, ×40). Micrograph (d) shows both primary and secondary follicles (F) stained with anti-CD79b antibody. Note that a large number of cells of the primary splenic nodules stained intensely with this B-cell antibody, whereas the mantle zone of secondary follicles contained the majority of CD79b-positive cells. Splenic nodules were often nestled between trabeculae (T) (Immunoperoxidase, ×40).

was associated with extensive lymphocyte infiltration into the surrounding red pulp and marked degradation of the splenic parenchyma.

GALT

Three samples of Mala intestine were inspected for the presence of GALT. One animal, acid-fast-positive animal 1, possessed a rim of lymphoid follicles along one side of the gut wall (Fig. 4a). The remaining two animals, acid-fast-negative 7 and 5, possessed distinct areas of longitudinal and circular muscle adjacent to the submucosa and clearly discernible blood vessels (Fig. 4b). The villi overlying this layer contained a capillary bed surrounded by a surface of columnar epithelial cells and small numbers of goblet cells. Small numbers of lymphocytes were also identified in the lamina propria of these samples, but both of these gut samples were devoid of obvious lymphoid aggregations.

A Peyer's patch was identified in the acid-fast-positive animal 1. In this animal, these lymphoid aggregations were present in the lamina propria, underlying the villi and were covered with a thin layer of epithelium. The Peyer's patch was composed of follicles with and without germinal centres that were joined by interfollicular areas composed predominantly of T cells as identified by anti-CD5 binding (Fig. 4c). CD5-positive cells were also detected inside the mantle zone of the germinal

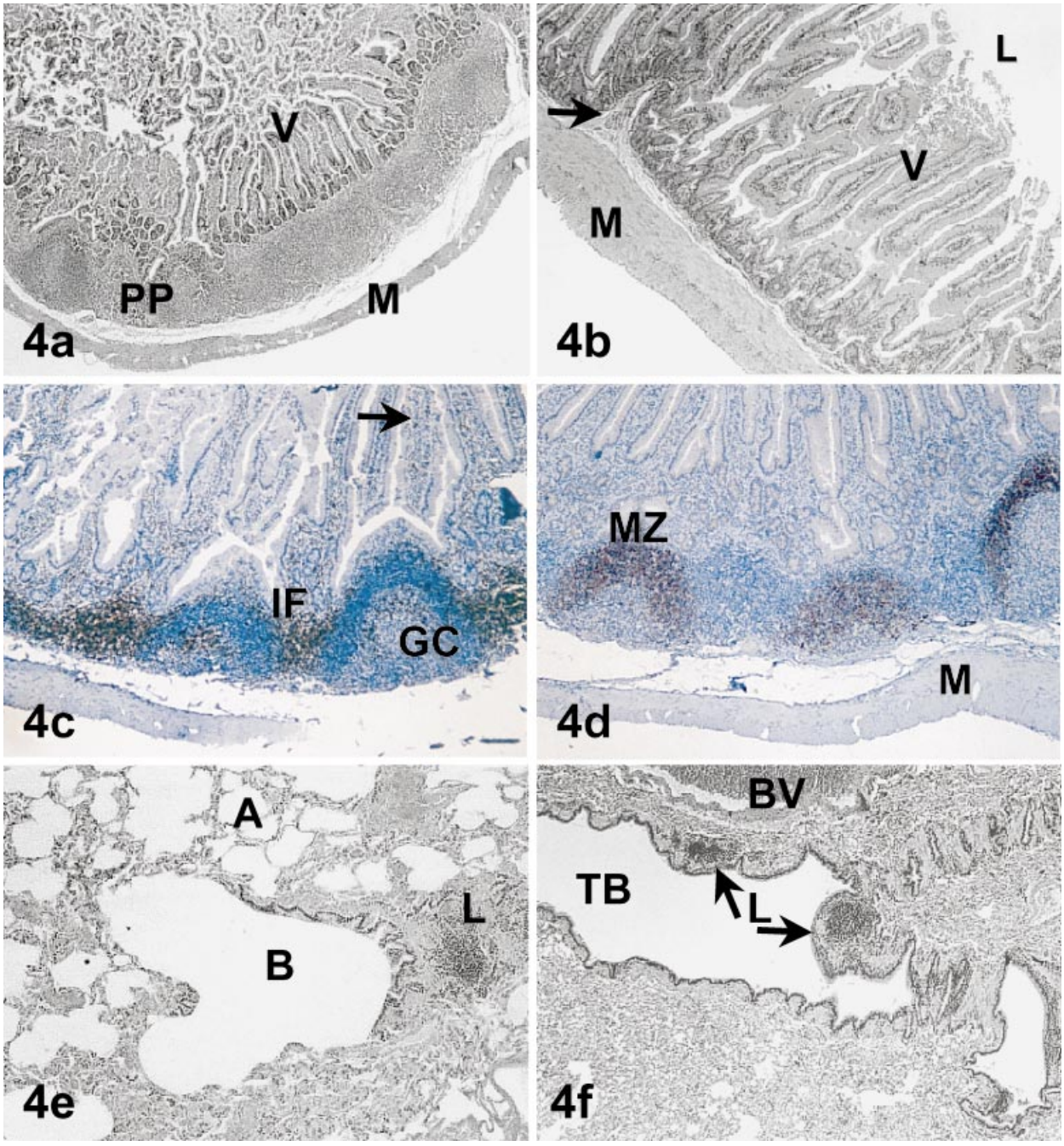

Fig. 4 Mala gut and bronchus-associated lymphoid tissue. In (a), a Peyer's Patch (PP) is visible between the villi (V) and the muscularis (M) (H&E, ×21). (b) A gut section devoid of lymphoid follicles. The details of the internal structure of villi (V) and the longitudinal and circular layers of the muscularis (M) can be clearly distinguished. A capillary (arrow) underlying the lamina propria is also visible in this section (H&E, ×40). (c,d) The T-cell and B-cell immunohistological staining of GALT, respectively. In (c), interfollicular (IF) cells stained strongly with anti-CD5 antibody along with some cells lining the luminal perimeter of the germinal centre (GC) and isolated cells within the villi (arrow). Cells within the GC did not stain with this antibody and were counterstained blue with haematoxylin (Immunoperoxidase, ×40). In (d), the mantle zone (MZ) of secondary follicles stained strongly with the B-cell antibody (anti-CD79b). Note the absence of B-cell staining in the interfollicular regions and within the villi (Immunoperoxidase, ×40). The follicles in both micrographs are positioned between the muscularis and lamina propria and have domes directed toward the gut lumen (L), which is not visible in (c) due to compression of the tissue prior to fixation. (e,f) Micrographs of Mala lung tissue containing lymphoid regions. In (e), a lymphoid aggregate (L) is positioned adjacent to a bronchiole (B). Alveoli (A) are visible in the surrounding tissue (H&E, ×100). In (f), two lymphoid nodules (L) are embedded in the walls of a tertiary bronchus (TB). Note the proximity of the large blood vessel (BV) (H&E, ×40).

centres and in scattered cells of the villi. Strong CD79b B-cell staining was evident in the mantle zones of the germinal centres and for almost all cells of the primary lymphoid follicles within the patch (Fig. 4d). Anti-CD79b antibody did not stain cells in the interfollicular areas and there was no detectable staining of cells with this antibody within the villi.

BALT

Organized regions of lymphoid tissue were detected in all samples of lung tissue inspected in this study. Lymphocyte aggregations were visible at the periphery of the bronchi and between the bronchi and blood vessels (Fig. 4e,f). Macrophages were present within the regions of BALT as well as in the alveoli and lung parenchyma. Fibrosis of the bronchial walls was evident in sections from acid-fast-positive animals 1, 3 and 5. In addition, large, multinucleated and epithelioid cells were commonly seen in the interalveolar regions of lung sections from animals 3 and 1. Foamy macrophages and neutrophils were also identified in the lung tissue of animal 1 along with a small number of focal non-caseating granulomas. The lung parenchyma and some alveoli from acid-fast-positive animal 2 contained a pink-staining proteinaceous fluid (H&E). Numerous infiltrating erythrocytes and lymphocytes were present and large air spaces resulting from collapsed alveoli were also visible in this sample. Similar cellular infiltrations were visible in the lung section of animal 6; however, whilst alveolar volume was reduced owing to the presence of increased cell numbers in the interalveolar spaces, the alveoli walls remained intact in this sample.

Despite a number of attempts, immunohistological identification of T and B cells in lung tissues was not possible due to non-specific staining of cuboidal epithelium lining the bronchial walls.

Discussion

Using opportunistically collected samples this study has documented the structure of lymphoid tissues of the Mala, including lymph nodes and spleen, GALT and BALT. Despite the obvious mycobacterial infection present in some of the animals studied, the structure of lymphoid tissues of the Mala resembled those of other macropod marsupials and are similar to those described for eutherian mammals. In animals that were identified as acid-fast positive it has also been possible to document some of the immunopathology associated with the presence of this disease agent.

Lymph nodes

The basic organization of lymph nodes included clearly demarked cortical and medullary regions enclosed by a fibrous capsule. Lymphoid follicles were situated in the outer regions of the node and were characterized by lighter staining germinal centres. This organization is similar to that described for other marsupials and most eutherian mammals with the exception of porcine species where the structure is inverted (Pabst & Binns, 1994). Consistent with reports of lymph node organization for other macropod species, the mantle of the secondary follicles contained predominantly B lymphocytes with T cells forming the major cell population in the paracortex (Hemsley et al. 1995; Old & Deane, 2001).

In the mesenteric lymph node of the clinically diagnosed and acid-fast-positive animal 1, the paracortical zone occupied an atypically large area of the node and contained predominantly T lymphocytes as evidenced by immunohistological staining. CD5-positive cells were densely distributed throughout the node, particularly in the cortical region and B-cell follicles were few in number. In humans, a nodal architecture similar to that described here, called paracortical hyperplasia, results from a predominantly cell-mediated response to viral infection. It is characterized by high numbers of parafollicular T lymphocytes that appear to 'push' small B-cell follicles to the periphery of the node (Burkitt et al. 1997). It would appear that exposure to mycobacteria results in similar responses in the Mala.

Spleen

The organization of the tissue bed of the Mala spleen was similar to that observed in eutherian mammals (Banks, 1981) with clearly distinguishable regions of white and red pulp infiltrated by numerous trabeculae. However, unlike human and bovine species, the Mala spleen contained extensive trabeculae that in some animals was fibrotic and in others was difficult to distinguish from lesions. The degree of fibrosis in these tissues is most likely associated with an immunological response. However, the observation of numerous trabeculae in all Mala spleen samples is consistent with observations by Hayes (1968) for another marsupial, the Virginia opossum (*Didelphis virginia*). Extensive trabeculae are

also found in some eutherian mammals where the spleen functions as a blood storage organ (Banks, 1981). As well as acting as a blood reservoir, the spleens of some animals also function to store platelets. The presence of megakaryocytes in Mala spleen is consistent with that observed in a variety of mammals such as rodents, felines and monotremes (Banks, 1981; Connolly et al. 1999) and suggests that platelet storage may also be a function of this organ in macropods.

In eutherian mammals, one of the primary functions of the spleen is to remove foreign matter, including bacteria, from blood flowing through the venous sinuses (Pabst & Binns, 1994). The localization of acid-fast bacteria within Mala spleen is therefore consistent with haematogenous spread of these pathogens. The spleens of disease-affected animals all demonstrated histopathological responses consistent with the presence of a pathogen carried by the circulatory route. Thickened blood vessel walls, extensive areas of white pulp surrounding arterioles, lymphocyte infiltration and the sequestering of acid-fast organisms by macrophages are all indications that the spleen of the Mala plays a major role in the eradication and clearance of antigen.

GALT

Whilst Peyer's patches have been described in a number of Australian marsupial species such as marsupial mice, *Antechinus swainsonii* and *A. stuartii* (Poskitt et al. 1984), koalas and two species of possum, *Trichosurus vulpecula and Pseudocheirus peregrinus* (Hanger & Heath, 1994; Hemsley et al. 1996), descriptions of GALT in adult macropod species are limited to two species, the Tammar wallaby (Hemsley et al. 1995; Old & Deane, 2002a) and the Eastern grey kangaroo *Macropus giganteus* (Old & Deane, 2001). In the Tammar wallaby, aggregations of lymphocytes were identified in the submucosa but no structured follicle aggregation such as a Peyer's patch was described (Basden et al. 1997). In contrast, in the Eastern grey kangaroo, GALT was identified as isolated lymphocytes within the villi and clearly defined Peyer's patches (Old & Deane, 2001). In the Mala, organized regions of aggregated follicles were not visible in all samples, but were present in the gut of one animal that was affected with mycobacteria. The presence of a Peyer's patch in the gut of this animal, together with the scattering of CD5-positive lymphocytes within the villi as well as in areas adjacent to the follicles, parallels the findings in *M. giganteus* and suggests that macropod species develop Peyer's patches in response to antigenic challenge.

BALT

BALT, identified as small aggregations of lymphocytes lining the bronchi or situated between the bronchi and a blood vessel, was identified in all animals in this study. Although in some species such as rabbits and rats, germ-free animals possess BALT, in humans and pigs, BALT arises in response to antigenic stimulation (Pabst & Binns, 1994). In the Mala, it is difficult to determine if these areas arose as a consequence of previous antigenic challenge or is endogenous.

Lung tissue from animal 1 contained multinucleated giant cells, cell types that are often found in association with mycobacterial infection (Burkitt et al. 1997). These cells have previously been reported in the lymph node of another macropod species, the Parma wallaby, *Macropus Parma*, in a case of mycobacterial osteomyelitis (Mann et al. 1982).

Immunopathology

Despite the susceptibility of marsupial species to mycobacterial disease (reviewed by Buddle & Young, 2000), the documentation of similar histological structures and the immunopathology associated with intracellular bacteria in this study has demonstrated that at least at the tissue bed level, the Rufous Hare-wallaby is able to mount an immune response that is similar to that described for eutherian mammals (reviewed by Thorel et al. 2001). There were obvious differences in the appearance of lymphoid tissues between healthy and diseased animals such as an increased paracortical region in the lymph node of animal 1 and the increased white pulp and large secondary follicles in the spleen of animal 5. However, there was no evidence of caseous necrosis often seen in advanced cases of mycobacterial infection in another marsupial, the brushtail possum (Cooke et al. 1995). However, copious cream-coloured pus was detected *post mortem* in an animal with fractured femurs resulting from osteomyelitis and osteoarthritis. The presence of multinucleated giant cells in the lung and the incidence of non-caseating granulomas are more consistent with responses to non-tuberculous mycobacteria from eutherian mammals (Cooke et al. 1995; Burkitt et al. 1997). Involvement of the spleen suggests haematogenous spread of the bacilli (Jackson

et al. 1995) and is consistent with the findings of generalized disease in these animals.

This is the first report describing the lymphoid tissues of the Rufous Hare-wallaby. As well as providing fundamental baseline information regarding the structure of the immune system in this species, this study has also confirmed that the techniques and reagents described herein are suitable for reviewing historical histological samples, since they are effective in paraffin-embedded tissue. This study also extends the range of species for which anti-CD5 and CD79b species cross-reactive antibodies can be utilized. It specifically provides fundamental information regarding the structure of the secondary lymphoid tissues in this endangered species and confirms that the Mala possesses the necessary cells and tissue organization consistent with the ability to generate a specific immune response. The phagocytosis of acid-fast bacteria by macrophages, the creation of large numbers of germinal centres, the presence of granulomatous lesions and the presence of GALT and MALT all suggest that this species possesses most of the sophistication associated with the immune systems of eutherian mammals.

Acknowledgments

We thank the Parks and Wildlife Commission of the Northern Territory and the Alice Springs Desert Park for access to material and Kim Branch for assistance in preparing samples. We thank Dr Margaret Jones of the Leukaemia Research Foundation (Oxford, UK) for the donation of antibodies and Anne Peck and Caroline Wilson for assistance with tissue processing. Lauren Young was supported by an Australian Postgraduate Award during this study.

References

Baker ML, Gemmell E, Gemmell RT (1999) Ontogeny of the Immune System of the Brushtail Possum, *Trichosurus vulpecula*. *Anat. Record* **256**, 354–365.

Bancroft JD, Stevens A (1990) *Theory and Practice of Histological Techniques*, 3rd edn. Edinburgh: Churchill Livingstone.

Banks WJ (1981) *Applied Veterinary Histology*. London: Williams & Wilkins.

Basden KE, Cooper DW, Deane EM (1997) Development of the lymphoid tissues of the tammar wallaby *Macropus eugenii*. *Reproduction, Fertil. Dev.* **9**, 243–254.

Bolton BL, Latz PK (1978) The Western Hare-wallaby, *Lagorchestes hirsutus* (Gould) (Macropodidae), in the Tanami Desert. *Aust. Wildlife Res.* **5**, 285–293.

Buddle BM, Young LJ (2000) Immunobiology of mycobacterial infections in Marsupials. *Dev. Comparative Immunol.* **24**, 517–529.

Burkitt HG, Stevens A, Lowe JS, Young B (1997) *Basic Histopathology*, 5th edn. Melbourne: Churchill Livingstone.

Canfield PJ, Hemsley S, Connolly J (1996) Histological and immunohistological study of the developing and involuting superficial cervical thymus in the koala (*Phascolarctos cinereus*). *J. Anat.* **189**, 159–169.

Celis JE (1994), ed. *Cell Biology*, Vol. 2. Sydney: Academic Press.

Cisternas PA, Armati PJ (2000) Immune system cell markers in the northern brown bandicoot, *Isoodon macrourus*. *Dev. Comparative Immunol.* **24**, 771–782.

Connolly JH, Canfield PJ, McClure SJ, Whittington RJ (1999) Histological and immunohistological investigation of lymphoid tissue in the platypus (*Ornithorhynchus anatinus*). *J. Anat.* **195**, 161–171.

Cooke MM, Jackson R, Coleman JD, Alley MR (1995) Naturally occurring tuberculosis caused by *Mycobacterium bovis* in brushtail possums (*Trichosurus vulpecula*). II. Pathology. *NZ. Vet. J.* **43**, 315–321.

Coutinho HB, Sewell HF, Tighe P, King G, Nogueira JC, Robalinho I, et al. (1995) Immunocytochemical study of the ontogeny of the Marsupial *Didelphis albiventris* immune system. *J. Anat.* **187**, 37–46.

Hanger JJ, Heath TJ (1994) The arrangements of gut-associated lymphoid and lymph pathways in the koala *Phascolarctos cinereus*. *J. Anat.* **185**, 129–134.

Hayes TG (1968) Studies of a primitive mammalian spleen, the opossum (*Didelphis virginiana*). *J. Morph.* **124**, 445–450.

Hemsley SW, Canfield PJ, Husband AJ (1995) Immunohistological staining of lymphoid tissue in four Australian marsupial species using species cross-reactive antibodies. *Immunol. Cell Biol.* **73**, 321–325.

Hemsley SW, Canfield PJ, Husband AJ (1996) Histological and immunohistological investigation of alimentary tract lymphoid tissue in the koala (*Phascolarctos cinereus*), brushtail possum (*Trichosurus vulpecula*) and ringtail possum (*Pseudocheirus peregrinus*). *J. Anat.* **188**, 279–288.

Jackson R, Cooke MM, Coleman JD, Morris RS (1995) Naturally occurring tuberculosis caused by *Mycobacterium bovis* in brushtail possums (*Trichosurus vulpecula*). I. An epidemiological analysis of lesion distribution. *NZ. Vet. J.* **43**, 306–314.

Johnson K (1988) Rufous Hare wallaby – rare and endangered. *Aust. Natural History* **22**, 406–407.

Jones M, Cordell JL, Beyers AD, Tse AGD, Mason DY (1993) Detection of T and B Cells in Many Animal Species Using Cross-Reactive Anti-Peptide Antibodies. *J. Immunol.* **150**, 5429–5435.

Kirsch JA, Lapointe FJ, Springer MS (1997) DNA-hybridisation Studies of Marsupials and their Implications for Metatherian Classification. *Aust. J. Zool.* **45**, 211–280.

Mann PC, Montali RJ, Bush M (1982) Mycobacterial osteomyelitis in captive Marsupials. *J. Am. Vet. Med. Association.* **181**, 1331–1333.

Mason DY, Cordell J, Brown M, Pallesen G, Ralfkiaer E, Rothbard J, et al. (1989) Detection of T cells in paraffin wax embedded tissue using antibodies against a peptide sequence from the CD3 antigen. *J. Clin. Pathol* **42**, 1194–1200.

Maxwell S, Burbidge AA, Morris K (1996) *Action Plan for Australian Marsupials and Monotremes*. Canberra: Wildlife Australia.

Old JM, Deane EM (2001) Histology and immunohistochemistry of the gut-associated lymphoid tissue of the eastern grey kangaroo, *Macropus giganteus*. *J. Anat.* **199**, 657–662.

Old JM, Deane EM (2002a) The gut associated lymphoid tissues of the northern brown bandicoot *Isoodon macrourus*. *Dev. Comparative Immunol*. **26**, 841–848.

Old JM, Deane EM (2002b) Immunohistochemistry of the lymphoid tissue of the tammar wallaby, *Macropus eugenii*. *J. Anat.* **201**, 257–266.

Pabst R, Binns RM (1994) The immune system of the respiratory tract in pigs. *Vet. Immunol. Immunopathol.* **43**, 151–156.

Poskitt DC, Duffey K, Barnett J, Kimpton WG, Muller HK (1984) The gut-associated lymphoid system of two species of Australian marsupial mice, *Antechinus swainsonii* and *Antechinus stuartii*. Distribution, frequency and structure of Peyer's patches and lymphoid follicles in the small and large intestine. *Aust. J. Exp. Biol. Med. Sci.* **62**, 81–88.

Thorel MF, Huchzermeyer HF, Michel AL (2001) *Mycobacterium avium* and *Mycobacterium intracellulare* infection in mammals. *Rev. Sci. Techn.* **20**, 204–218.